COMPDYN 2011
3rd ECCOMAS Thematic Conference on
Computational Methods in Structural Dynamics and Earthquake Engineering
M. Papadrakakis, M. Fragiadakis, V. Plevris (eds.)
Corfu, Greece, 25–28 May 2011

# EFFICIENT MODEL UPDATING OF THE GOCE SATELLITE BASED ON EXPERIMENTAL MODAL DATA

**B. Goller[1], M.Broggi[1], A. Calvi[2] and G.I. Schuëller[1]**

[1]Institute of Engineering Mechanics, University of Innsbruck
Technikerstr. 13, 6020 Innsbruck, Austria, EU
e-mail: mechanik@uibk.ac.at

[2] Structures Section TEC-MSS, European Space Agency / ESTEC
P.O. Box 299, 2200 AG Noordwijk, The Netherlands, EU
e-mail: adriano.calvi@esa.int

**Keywords:** Model updating, model validation, uncertainty quantification, model reduction

**Abstract.** *The accurate prediction of the structural response of spacecraft systems during launch and ascent phase is a crucial aspect in design and verification stages which requires accurate numerical models. The enhancement of numerical models based on experimental data is denoted model updating and focuses on the improvement of the correlation between finite element (FE) model and test structure. In aerospace industry the judgment of the agreement between model and real structure involves the comparison of the modal properties of the structure. Model updating techniques have to handle several difficulties, like incomplete experimental data, measurement errors, non-unique solutions and modeling uncertainties. To cope with the computational challenges associated with the large-scale FE-models involving up to over one million degrees of freedom (DOFs), enhanced strategies are required. A large-scale numerical example, namely a satellite model, will be used for demonstrating the applicability of the employed updating procedure to complex aerospace structures.*

## 1 INTRODUCTION

The dynamic loads acting on a spacecraft during the launch and ascent phase are modeled by the spacecraft-launcher coupled dynamic analysis. The accuracy of the structural response in this low-frequency mechanical environment depends on the quality of the underlying mechanical model of the spacecraft. Therefore, it is mandatory to ensure that the FE-model represents the real structure accurately enough. This level of accuracy to be reached for aerospace structures is defined in [1] and is based on the agreement of experimentally and computationally determined modal properties, respectively. Possible sources for discrepancies between test data and respective computed values are e.g. uncertainties in the modeling process arising from inadequate theory for some system behaviors, simplifying assumptions made in order to reduce the complexity of the model and uncertainties about model parameter values. Hence, the need for improving the mechanical model based on experimental data arises which is referred to as model updating and the consecutive corroboration of the model by means of modal properties is denoted by validation [2, 3, 4].

The use of deterministic updating procedures does not allow for a quantification of the involved uncertainties in the design and verification processes which will subsequently affect the accuracy of the predictive structural response. Probabilistic methods for model updating provide a means for tackling these problems and for avoiding a wrong conclusion about the fit of the experimental data and analytical results [5]. A significant obstacle in the consideration of uncertainties when performing model updating of complex structures is posed by the associated computational efforts. Therefore, the most frequently used approaches for model updating performed by industry are deterministic approaches (see e.g. [6, 7, 8, 9]). While stochastic methods have been developing successfully in this research field, applications in industry are relatively limited (see e.g. [10]). Hence, in this work it is aimed at a computationally efficient application of a stochastic model updating procedure to complex aerospace models.

The thereby adopted updating process is the Bayesian approach which is based on updating the initial engineering knowledge about the ranges of the adjustable parameters using experimental data [11, 12, 13]. In this way, a revised information about the parameters is obtained, which is expressed by posterior probability density functions. Probability is therefore not interpreted in the usual frequentist sense, where it refers to the relative frequency of occurrence in case of many events, but it is based on the idea of reasonable expectation, i.e. probability is interpreted as a measure of plausibility of the hypothesis. This interpretation makes it possible to extend the application of probability theory to fields where the frequentist interpretation may not be directly intuitive, as it is the case for one-of-a-kind structures, where no ensemble exists, and also in the case of limited data, where classical statistics is of limited applicability. Therefore, Bayesian statistics makes it possible to deal with the usual situation in aerospace industry, where a large amount of experimental data is infeasible due to the enormous costs associated with test campaigns, and it provides a means for making decisions based on limited, incomplete information.

The computational tools for the Bayesian updating procedure are sampling-based algorithms, where a multi-level Markov chain Monte Carlo algorithm is adopted in this approach [14]. As a remedy for the large computational efforts associated with the Bayesian updating procedure, the application of a surrogate model (a so-called “meta-model”) is proposed. This meta-model

is formulated with respect to the repeated analysis tasks, which are the eigensolutions in case of model updating based on modal data. Hence, a simple relation between the input data and output quantity of interest has to be established in order to replace the computationally intensive evaluation of a full finite element analysis by a function evaluation at low computational costs. Several techniques, e.g. linear or polynomial regression, kriging and the radial basis functions have been developed in this context (see e.g. [15]), where in this work neural networks [16] will be adopted in order to approximate the modal properties of the structure.

This manuscript will demonstrate the feasibility of the application of Bayesian model updating procedures on spacecraft structures using eigenfrequencies and mode shape vectors. Sec. 2 is devoted to the presentation of the basic steps of Bayesian model updating, and in Sec. 3 the algorithm for the generation of samples in the solution space is summarized. Computational aspects will be addressed in the following (Sec. 4), where the basic concepts of neural networks are discussed. In order to apply these outlined concepts to an FE-model of a spacecraft structure, the use of a surrogate model within the updating process is adopted for the FE-model of the GOCE satellite (Sec. 5).

## 2 BAYESIAN MODEL UPDATING

### 2.1 Introduction

The fundamental rule that governs the Bayesian updating procedure is Bayes' Theorem, which is formulated in general terms as [17]

$$P(H|\mathcal{D},I) = \frac{P(\mathcal{D}|H,I)P(H|I)}{P(\mathcal{D}|I)}, \tag{1}$$

where $H$ is any hypothesis to be tested, $\mathcal{D}$ denotes the data and $I$ is the available background information. Bayes' Theorem provides a means to update the prior probability density function (PDF) of $H$, $P(H|I)$, by using the data in the likelihood function $P(\mathcal{D}|H,I)$ in order to obtain the posterior distribution of $H$, $P(H|\mathcal{D},I)$. The denominator $P(\mathcal{D}|I)$ is a normalizing constant and does not affect the shape of the posterior PDF. All probabilities in Eq. (1) are conditional on $I$, which means that the outcome of the updating procedure depends on the available information.

### 2.2 Bayesian updating using modal data

If applying Bayes' Theorem for structural model updating [11, 12], the hypothesis $H$ is interpreted as the vector of unknown (i.e. adjustable) parameters, which will be referred to as $\theta$ in the following, and $\mathcal{D}$ denotes the experimental data, which consist of the measured modal properties of the investigated structure. The available information $I$ is interpreted as the experience and knowledge of the engineer which is reflected by the established model itself and is therefore denoted as $\mathcal{M}$. This leads to the following form of Eq. (1):

$$p(\theta|\mathcal{D},\mathcal{M}) = \frac{p(\mathcal{D}|\theta,\mathcal{M})p(\theta|\mathcal{M})}{p(\mathcal{D}|\mathcal{M})}. \tag{2}$$

The prior distribution $p(\theta|\mathcal{M})$ expresses the initial knowledge about the adjustable parameters. The choice of the distribution can be based on the principle of maximum entropy [18]. In this

case, the PDF used for describing the initial uncertainty maximizes the uncertainty subject to the prescribed constraints, which can be given by e.g. imposing moment constraints. The likelihood function $p(\mathcal{D}|\theta, \mathcal{M})$ gives a measure of the agreement between the system data and the corresponding structural model output. This measure of the data fit of each model defined by the parameters vector $\theta$, is given by the probability model established for the system output. The derivation of the likelihood function for modal data will be summarized in Sec. 2.3. The posterior distribution $p(\theta|\mathcal{D}, \mathcal{M})$ expresses the revised knowledge about the parameters $\theta$ conditional on the initial knowledge and the experimental data.

### 2.3 Formulation of the likelihood function for modal data

In general terms, the connection between the model output $q(\theta)$ and the corresponding system output $y$ is given by the prediction error $e$ in the form of

$$y = q(\theta) + e. \tag{3}$$

The choice for the probability model of the prediction error $e$, which is the difference between the model output for a certain value of $\theta$ and the corresponding system output, is based on the maximum entropy principle [18] which yields a multi-dimensional Gaussian distribution with zero mean and covariance matrix $\Sigma$. The Gaussian PDF arises because it gives the largest amount of uncertainty among all probability distributions for a real variable whose first two moments are specified. Hence, the predictive PDF for the system output conditional on the parameter vector $\theta$ is given by

$$p(y|\theta, \mathcal{M}) = \frac{1}{(2\pi)^{N/2}|\Sigma|^{1/2}} \exp\left[-\frac{1}{2}(y - q(\theta))^T \Sigma^{-1}(y - q(\theta))\right], \tag{4}$$

where $N_0$ $N$ denotes the length of the vector $y$, i.e. the number of observed points. If a set of measured output $\mathcal{D} = \{y_j : j = 1, \ldots, N_s\}$ is available, then the likelihood function can be constructed as $p(\mathcal{D}|\theta, \mathcal{M}) = \prod_{j=1}^{N_s} p(y_j|\theta, \mathcal{M})$ if the prediction errors are modeled as statistically independent.

The formulation of the likelihood function using modal data is derived in [19] and is summarized in the following. The experimental data $\mathcal{D}$ from the structure is assumed to consist of $N_s$ sets of modal data, $\mathcal{D} = \{\hat{\omega}_{1,j} \ldots \hat{\omega}_{N_m,j}, \hat{\Psi}_{1,j} \ldots \hat{\Psi}_{N_m,j}\}_{j=1}^{N_s}$ comprised of $N_m$ modal frequencies $\hat{\omega}_r$ and $N_m$ incomplete mode shape vectors $\hat{\Psi}_r \in \mathbb{R}^{N_0}$, where $N_0$ is the number of observed DOFs. The model output $q(\theta)$ is the set of corresponding modal properties of the structural model, i.e. eigenfrequencies $\omega_r(\theta)$ and partial eigenvectors $\psi_r(\theta)$, $r = 1, \ldots, N_m$, defined by the parameter vector $\theta \in \Theta \in \mathbb{R}^{N_p}$.
The probability model conditional on the parameter vector $\theta$ is chosen to have statistical independence between the mode shape vectors and modal frequencies, between the different modes, and between one data set to another. Therefore, the likelihood function can be written as the product of the probability density functions for the modal frequencies and mode shape components:

$$p(\mathcal{D}|\theta, \mathcal{M}) = \prod_{j=1}^{N_s} \prod_{r=1}^{N_m} p(\hat{\omega}_{r,j}^2|\theta, \mathcal{M}) p(\hat{\psi}_{r,j}|\theta, \mathcal{M}), \tag{5}$$

where $p(\hat{\omega}_{r,j}^2|\theta, \mathcal{M})$ and $p(\hat{\psi}_{r,j}|\theta, \mathcal{M})$, $r = 1, \ldots, N_m$ and $j = 1, \ldots, N_s$, are, respectively, the PDFs for the squared modal frequency and the mode shape vector of the $r$th mode in the $j$th

data set.

In the first step, the likelihood function for the mode shape vectors is formulated by rewriting Eq. (3) as

$$\hat{\psi}_{r,j} = a_r \psi_r(\theta) + e_{\psi_r}, \tag{6}$$

where $a_r$ is an optimal scaling factor to relate the scaling of the model mode shape vector $\psi_r(\theta)$ to that of the experimental mode shape vector $\hat{\psi}_{r,j}$, which is assumed to be normalized so that its Euclidean norm $\|\hat{\psi}_{r,j}\| = 1$. Since the latter is usually constituted by an incomplete set of observed DOFs $N_0$, the corresponding model mode shape vector is given by $\psi_r = \Gamma\phi_r$ , where the matrix $\Gamma$ picks the observed degrees of freedom from the complete model eigenvector $\phi_r$. Using a Gaussian distribution for the probabilistic characterization of the prediction error for the mode shape vector, the likelihood function for the mode shape vector, after some algebraic manipulation, may be written as:

$$p(\hat{\psi}_{r,j}|\theta, \mathcal{M}) = c_1 \exp\left(\frac{\psi_r^T (I - \hat{\psi}_{r,j}\hat{\psi}_{r,j}^T)\psi_r}{2\delta_r^2 \|\psi_r\|^2}\right) \tag{7}$$

$$= c_1 \exp\left(\frac{1}{2\delta_r^2}\left[1 - \frac{|\psi_r^T \hat{\psi}_{r,j}|^2}{(\psi_r^T \psi_r)^2}\right]\right) \tag{8}$$

where $I$ is the identity matrix of dimension $N_m$ and $\delta_r^2 I$ denotes the mode shape prediction error covariance matrix for the $r$th mode. The equality in Eq. (8) shows that the probability density function for $\hat{\psi}_{r,j}$ involves the MAC (Modal Assurance Criterion) between $\hat{\psi}_{r,j}$ and $\psi_r(\theta)$, the experimental and model partial mode shapes of the $r$th mode, respectively.

Secondly, Eq. (3) is formulated for the squared modal frequencies, which yields

$$\hat{\omega}_{r,j}^2 = \omega_r^2(\theta) + e_{\omega_r^2}. \tag{9}$$

Using again a Gaussian probability model for the prediction error of the modal frequencies, the likelihood function for the modal frequencies is given by

$$p(\hat{\omega}_{r,j}^2|\theta, \mathcal{M}) = c_2 \exp\left[-\frac{1}{2}\left(\frac{1 - \hat{\omega}_{r,j}^2/\omega_r^2}{\varepsilon_r}\right)^2\right], \tag{10}$$

where $\varepsilon_r^2$ denotes the variance of the prediction error of the squared $r$-th eigenfrequency, i.e. of $e_{\omega_r^2}$. Using the probability distributions for the mode shape vectors and modal frequencies given in Eqs. (8) and (10), the likelihood function in Eq. (5) can be written as

$$p(\mathcal{D}|\theta, \mathcal{M}) = c_3 \exp\left(-\frac{1}{2}\sum_{r=1}^{N_m} J_r(\theta)\right), \tag{11}$$

where the modal measure of fit $J_r(\theta)$ is defined by

$$J_r(\theta) = \sum_{j=1}^{N_s}\left[\left(\frac{1 - \hat{\omega}_{r,j}^2/\omega_r^2}{\varepsilon_r}\right)^2 + \left(1 - \frac{|\psi_r^T \hat{\psi}_{r,j}|^2}{(\psi_r^T \psi_r)^2}\right)/\delta_r^2\right] \tag{12}$$

## 3 TRANSITIONAL MARKOV CHAIN MONTE CARLO ALGORITHM

The evaluation of Eq. (2) requires the computation of high-dimensional integrals for the determination of the normalizing constant of the posterior PDF, which cannot be tackled analytically or numerically. Recently, efficient stochastic simulation algorithms have been proposed which generate samples of the posterior distribution and which hence identify the parameter regions with the highest posterior probability mass. In this work, the so-called Transitional Markov Chain Monte Carlo (TMCMC) algorithm [14] is applied whose basic steps are discussed in the following.

The main idea of this algorithm is to iteratively proceed from the prior to the posterior distribution. It starts with the generation of samples from the prior PDF in order to populate the space in which also the most probable regions of the posterior distribution lie. Then, some intermediate PDFs are defined, where the shape does not change remarkably from the intermediate PDF $p[j]$ to the next $p[j+1]$. The small change of the shape makes it possible to efficiently sample according to $p[j+1]$ if samples according to $p[j]$ have been generated. The intermediate distributions are defined by

$$p[j+1] \propto p(\mathcal{D}|\theta,\mathcal{M})^{\beta_j} p(\theta|\mathcal{M}), \tag{13}$$

with $j = 0, \dots m$ as the step index and $0 = \beta_0 < \beta_1 < \ldots < \beta_m = 1$. Hence, the exponent $\beta_j$ can be interpreted as the percentage of the total information provided by the experimental data which is incorporated in the $j$th iteration of the updating procedure: $\beta_0 = 0$ corresponds to the prior distribution and for $\beta_m = 1$ the samples are generated from the posterior distribution.

Samples of the subsequent intermediate distribution $p[j+1]$ are obtained by generating Markov chains where the lead samples are selected from the distribution $p[j]$ by computing their probability weights with respect to $p[j+1]$, which are given by

$$w(\theta_j^{(l)}) = \frac{p(\mathcal{D}|\theta,\mathcal{M})^{\beta_{j+1}} p(\theta|\mathcal{M})}{p(\mathcal{D}|\theta,\mathcal{M})^{\beta_j} p(\theta|\mathcal{M})} = p(\mathcal{D}|\theta,\mathcal{M})^{\beta_{j+1}-\beta_j}, \tag{14}$$

where the upper index $l = 1, \dots, N_j$ denotes the sample number in the $j$th iteration step. Each sample of the current step is generated using the Metropolis-Hastings algorithm [20, 21]: the starting point of a Markov chain is a sample from the previous step that is selected according to the probability equal to its normalized weight

$$\overline{w}(\theta_j^{(l)}) = \frac{w(\theta_j^{(l)})}{\sum_{l=1}^{N_j} w(\theta_j^{(l)})} \tag{15}$$

and the proposal density for the Metropolis-Hastings algorithm is a Gaussian distribution centered at the preceding sample of the chain and with a covariance matrix $\Sigma_0$ which is equal to the scaled version of the estimated covariance matrix of the current intermediate PDF:

$$\Sigma_0 = c^2 \sum_{l=1}^{N_j} \overline{w}(\theta_j^{(l)})(\theta_j^{(l)} - \overline{\theta}_j)^T(\theta_j^{(l)} - \overline{\theta}_j), \tag{16}$$

where

$$\overline{\theta}_j = \sum_{l=1}^{N_j} \overline{w}(\theta_j^{(l)})\theta_j^{(l)}. \tag{17}$$

The parameter $c$ is a scaling parameter that is used to control the rejection rate of the Metropolis-Hastings algorithm at each step. These steps are repeated until $\beta_j = 1$ is reached, i.e. until the samples are generated from the posterior distribution.

# 4 COMPUTATIONAL ASPECTS

## 4.1 General remarks

Due to the repeated execution of the normal mode analysis of the FE-model, the computational effort of the Bayesian updating method might become infeasible for large FE-models. Hence, in order to reduce the wall clock time, i.e. the time between submitting the updating analysis and its completion, a strategy based on the reduction of the computational efforts associated with the normal mode analysis of the full FE-model is applied in this manuscript. This strategy is based on the use of neural networks for the modal parameters, which will be addressed in the following.

## 4.2 Neural networks

An Artificial Neural Network (ANN) is a machine-learning algorithm that tries to simulate the structure and functional aspects of biological networks of neurons in order to approximate a relation $f : \theta \rightarrow q$ by a simple mathematical model at low computational efforts. It consists of an interconnected group of computational units, called neurons or nodes, and processes information using consecutively connected layers of neurons. In the following, the most widely used neural network, namely the so-called feed-forward neural network, is discussed (see e.g. [22, 23]). It is composed of a multi-layered structure, with a first layer of nodes, called input layer, one or more intermediate layers, called hidden, and a final output layer. For simplicity, but without loss of generality, the scheme is discussed when using one single hidden layer.

Each layer is characterized by a different number of neurons, indicated by $N_{inp}$, $N_{hid}$ and $N_{out}$ for the input, hidden and output layers, respectively. Each node of the hidden layer receives as input a linear combination $\sum_{i=1}^{N_{inp}} w_{i,j}\theta_i$ of the input values $\theta_i$ of all the nodes of the input layer, scaled by a so-called connection weight $w_{i,j}$, where $j$ denotes the number of the hidden node. Then, the node proceeds this function value through a non-linear function $K$, which is called activation function and which is of the form $g_j = K(\sum_{i=1}^{N_{inp}} w_{i,j}\theta_i)$. This collection of function values $(g_1, \ldots, g_{N_{hid}})$ is then sent to all the nodes of the subsequent, i.e. output, layer, where the approximated model output $\hat{q}_k(\theta) = K(\sum_{j=1}^{N_{hid}} w_{j,k}y_j))$, $k = 1, \ldots N_{out}$ is evaluated. A schematic representation of this algorithm is shown in Fig. 1.

Hence, the connection weights act as parameters of the meta-model which have to be adapted through a calibration procedure of supervised learning, called also training, by means of e.g. the error back-propagation algorithm. In this calibration phase, the network, which is initialized with random weights, is fed with a set of input/output values which is called calibration set and which is obtained from the target physical model. The network processes the inputs and produces then an estimation of the outputs; such outputs are compared with the real outputs through a predefined error measurement (typically, a sum of the squared errors of each output). The training consists thus of an optimization problem which aims to minimize the error of the network in the output prediction. Such optimization is carried out by computing the gradient of the error with respect to the connection weights, and it is interrupted when a target error is reached or when a certain number of input/output pairs have been processed.

An important indicator of the goodness of the network after training is the coefficient of

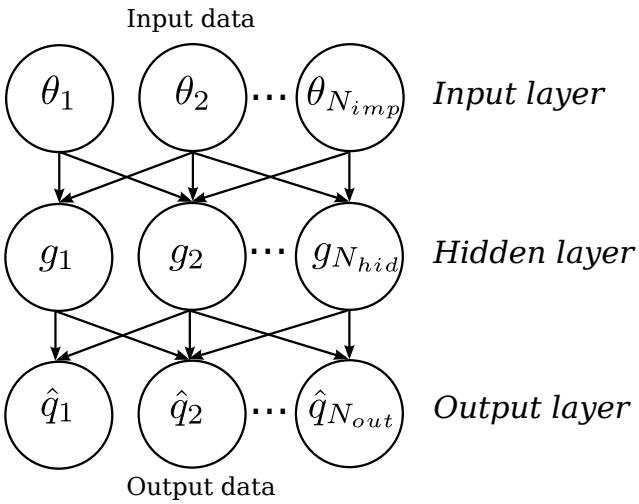


Figure 1: Schematic representation of the concept of neural networks

determination $R^2$, defined as

$$R^2 = 1 - \frac{\sum_{i=1}^{N_{data}} (q_i - \hat{q}_i)^2}{\sum_{i=1}^{N_{data}} (q_i - \overline{q}_i)^2} \tag{18}$$

where $q_i$ are the real outputs of the physical model, $\overline{q}_i = \frac{1}{N_{data}} \sum_{i=1}^{N_{data}} q_i$ and $\hat{q}_i$ are the output values predicted by the meta-model. The accuracy of the output prediction of the neural network can be judged by the closeness of the value $R^2$ to the target value of 1.0, which expresses an exact match of the network prediction and the output of the full model. This quantity is computed both using the calibration set and a new set of input/output values, called validation or verification set. In the latter case, a qualitative indication of the generalization capabilities of the network is obtained.

The freely available Fast Artificial Neural Network (FANN) library [24], which is an implementation of the here discussed Neural Network and learning algorithm, has been used for the approximation of the modal properties in the following numerical example.

## 5 NUMERICAL EXAMPLE: GOCE SATELLITE

### 5.1 Problem statement

The use of a meta-model within the Bayesian updating procedure is illustrated using the Gravity Field and Steady-State Ocean Circulation Explorer (GOCE) satellite. The mission of the GOCE satellite is to determine the geoid and to measure the gravitational field of Earth with a very high degree of accuracy in a low Earth orbit. The particularities of the GOCE are its arrow-shape with winglets and its ion propulsion engine, used to compensate the air-drag induced orbit-decay. The total length of the satellite is 5.3 m, and the mass amounts to approximately 1,000 kg including the fuel of the propulsion system.

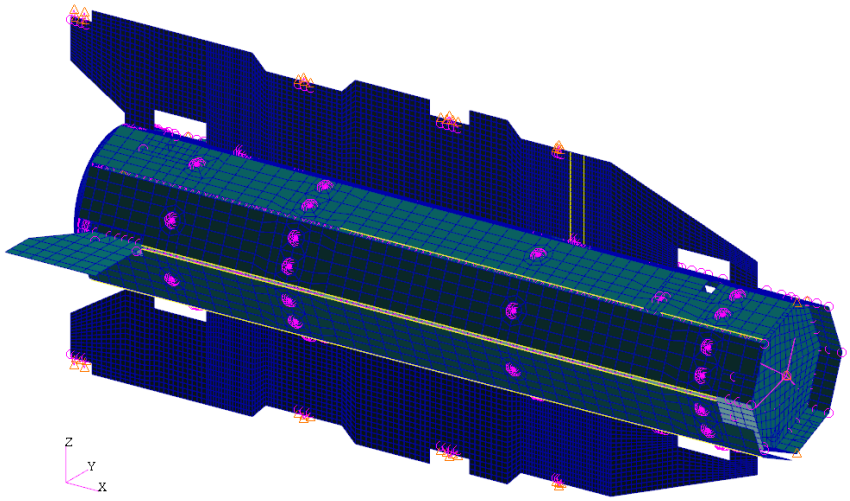


Figure 2: FE model of the GOCE satellite (courtesy of Thales Alenia Space Italy)

Fig. 2 shows the FE model of the satellite, provided by Thales Alenia Space (Italy) for use within the commercial FE code MSC.Nastran [25]. Approximately 360,000 DOFs and 74,000 elements compose the FE model, with half of the elements used in the main satellite platform and half in the gravitational gradiometer.
In the main GOCE platform, quadrilateral (QUAD4) and triangular (TRIA3) shell elements are used to model the body panels, the wings and the winglets, the internal floors and the solar panels. Beam elements (BAR, ROD and BEAM) constitute the connections of the wings to the main structure and of the instrumentation to the floors. Solid elements (HEXA and PENTA) are used in the Launch Vehicle Adapter (LVA) ring, and scalar spring elements (CELAS2) represent the connection between the solar panels and the structure, as well as the fixing of the wing to the main octagonal body.

A total number of 18 groups combining 3047 structural parameters are defined according to the type and location of the respective materials or geometric specifications (see Tab. 1). This grouping is carried out with the purpose of remarkably reducing the number of parameters to be used within the Bayesian updating procedure since an independent processing of all involved parameters might become infeasible. Hence, the updating procedure is carried out with the goal of identifying as to which changes have to be performed to the single parameter groups in order to obtain a better agreement of the numerical model with the real satellite structure.

### 5.2 Experimental modal data

The experimental data used for model updating consists of $N_s = 1$ set of 7 modal frequencies and partial mode shapes vectors (83 components) which have been determined from the vibration responses during the GOCE structural model qualification test. The dynamic qualification test was performed on the multi-axis vibration test facility of ESA/ESTEC in Noordwijk (The Netherlands). The correlation of the experimental and computed eigenvectors of the initial model is shown by means of the MAC matrix in Fig. 3 and the initial comparison of the eigenfrequencies can be found in Tab. 2. The large discrepancies, especially for the first two modes,

| Group no. | Parameters |
|---|---|
| 1 | Young's modulus of isotropic materials |
| 2 | Poisson's ratio of isotropic materials |
| 3 | Young's modulus in the principal direction of orthotropic materials |
| 4 | Young's modulus in the secondary direction of orthotropic materials |
| 5 | Poisson's ratio of orthotropic materials |
| 6 | In-plane shear modulus of orthotropic materials |
| 7 | First out-of-plane shear modulus of orthotropic materials |
| 8 | Second out-of-plane shear modulus of orthotropic materials |
| 9 | Densities of the materials |
| 10 | Thicknesses of the shells |
| 11 | Linear elastic connections of panels to the main satellite structure |
| 12 | Linear elastic connections of panels to the satellite wings |
| 13-18 | Linear elastic connections of the wings to the main satellite structure |

Table 1: Definition of the groups of parameters of the GOCE satellite

arise the need for model updating which will be discussed in the following.

| Mode no. | $f_a$ [Hz] | $f_e$ [Hz] | $\Delta$ [%] |
|---|---|---|---|
| 1 | 18.43 | 15.98 | 13.29 |
| 2 | 18.37 | 16.40 | 10.69 |
| 3 | 28.84 | 29.59 | -2.60 |
| 4 | 34.96 | 33.33 | 4.66 |
| 5 | 46.90 | 48.91 | -4.28 |
| 6 | 49.13 | 51.61 | -5.04 |
| 7 | 65.81 | 61.35 | 6.77 |

Table 2: Comparison of the analytical eigenfrequencies $f_a$ and the experimental data $f_e$

### 5.3 Accuracy analysis of the neural network

A set of $N_{data} = 2,000$ finite element simulations have been performed using Gaussian distributions with the mean values equal to the nominal values and coefficients of variation of 10%. Out of these samples, 1,900 have been dedicated to calibrate the neural networks, and 100 have been kept to verify the generalization capabilities of the networks after training. Each of the 14 neural networks, constituted by $N_{inp} = 18$ inputs and $N_{out} = 1$ output, predicts either one of the eigenfrequencies or one of the diagonal terms of the MAC matrix.
An automated training procedure has been implemented such that various network topologies are tested and the best networks, characterized by the highest $R^2$ value (see Eq. (18)) obtained with the verification data, are kept. As an indication of the accuracy of the network, Fig. 4 shows the regression plots for the neural network of the first eigenfrequency, using the calibration and verification data, respectively. Moreover, the values of $R^2$ of all the networks obtained with the verification data are listed in Tab. 3.

### 5.4 Bayesian model updating

The prior distributions assigned to the 18 groups of parameters to be updated are all Gaussian with the moments as specified for the calibration of the neural networks. For these ranges, the

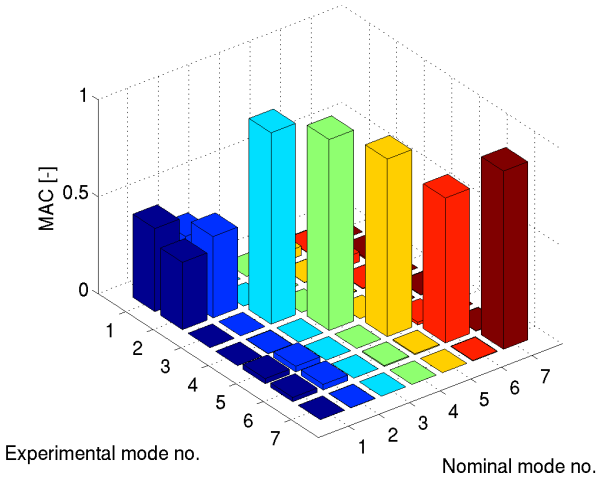


Figure 3: Initial MAC values obtained with the nominal model and the experimental data $\hat{\psi}$

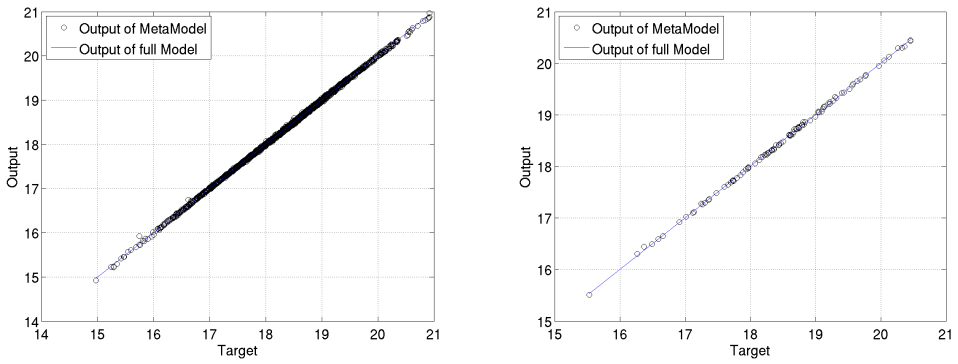


(a) (b)

Figure 4: Regression plot of the output of the neural network of the first eigenfrequency for (a) calibration data and (b) verification data.

| Neural network output | $R^2$ of verification data |
|---|---|
| Frequency 1 | 0.99960 |
| Frequency 2 | 0.99966 |
| Frequency 3 | 0.99968 |
| Frequency 4 | 0.99957 |
| Frequency 5 | 0.88299 |
| Frequency 6 | 0.97804 |
| Frequency 7 | 0.95822 |
| $MAC_{1,1}$ | 0.99886 |
| $MAC_{2,2}$ | 0.99782 |
| $MAC_{3,3}$ | 0.99577 |
| $MAC_{4,4}$ | 0.99861 |
| $MAC_{5,5}$ | 0.94947 |
| $MAC_{6,6}$ | 0.97623 |
| $MAC_{7,7}$ | 0.82779 |

Table 3: $R^2$ values of the 14 neural networks

neural networks of the considered modal properties show high accuracy as discussed in the previous section and are therefore applied for substituting the full FE-analysis when evaluating the likelihood function within the updating process.
The results of the updating procedure are shown exemplarily for three parameter groups, namely the thickness, the Young's moduli of the orthotropic materials and the group of stiffnesses of joints between the wings and the main structure (groups no. 10, 3 and 14 in Tab. 1). The prior and posterior histograms of these parameters, which are all transformed in standard normal space, are depicted in Figs. 5-7. This representation in standard normal space is advantageous due to the fact that these figures do not show one single parameter each but a parameter group, where the members of each group may have different initial values. Hence, in order to obtain the posterior values in physical space, a back-transformation has to be performed for each parameter of a group, which is achieved by

$$\theta_i = \theta_i^* \sigma_i + \theta_{i,\mathrm{nom}}, \tag{19}$$

where $\theta_i$ denotes the $i$-th parameter in the physical space, $\theta_i^*$ the value in the standard normal space, $\sigma_i$ the prior standard deviation and $\theta_{i,\mathrm{nom}}$ the prior (nominal) mean of this parameter.

In Fig. 5, the prior and posterior histograms of the thickness of shell elements are depicted. This figure leads to the conclusion that the information contained in the experimental data suggests a decrease of these values. A reduction of approximately 10% of the mean value of the prior distribution leads to a better fit with the experimental modal properties. Also for the Young's modulus of the orthotropic material in the longitudinal direction (material card MAT8 in the MCS.Nastran input file), the updating process suggests a decrease of the mean values (see Fig. 6). As opposed to these two parameter groups, all other 16 out of 18 parameter groups used in the updating process show small changes if compared to the prior distribution. As an example, the stiffness values of the joints of the main structure to the wings (used for the specification of the CELAS2 elements in the MCS.Nastran input file) is shown in Fig. 7. Due to the information extracted from the experimental values, the prior uncertainty about these parameters could be reduced which is visible through the smaller variation of the posterior distribution.

The effect of the choice of the prior on the posterior distribution has not been investigated in this example, however a few remarks will be added in this context: in general, the influence

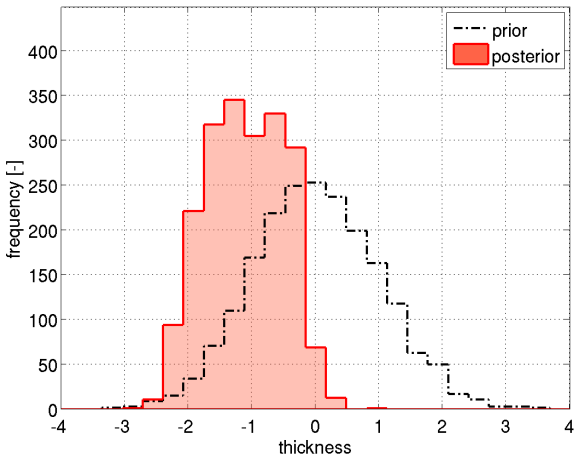


Figure 5: Histograms of the prior and posterior samples of the group of thicknesses (group no. 10 in Tab. 1)

of the prior distribution on the results decreases with increasing amount of experimental data. This is due to the fact that the likelihood function becomes the dominant term in comparison to the prior distribution in Eq. (2). In this case, also values in the tails of the prior distribution can be identified and only values with zero probability (e.g. values out of the interval of uniform distributions) cannot be reached since they are excluded from the possible solution space due to the prior knowledge. In case of limited data the selection of the prior distribution clearly has an influence on the results. The prior distribution can therefore be seen as a means to incorporate initial knowledge about parameter ranges into the identification process and it is subjective in the sense that people with different experience may use different priors leading to broader ranges of the solution in case smaller amount of prior information is available. The selection can therefore be seen as part of the modeling process since also the model itself is affected by a certain amount of subjectivity of the designer. However, the probability content of the prior PDF is updated by the data and if one felt uncomfortable with the choice of the prior distribution the effect of different prior PDFs on the posterior PDF can be studied.

### 5.5 Effect on the correlation of modal data

The effect of the updating procedure on the correlation of the experimental and computed modal properties is shown exemplarily for the two lowest and highest considered modes. Figs. 8-11 are devoted to the eigenfrequencies and Fig. 12 to the corresponding diagonal MAC-values. The figures show that a successful shift of the PDFs towards the experimental values could be achieved, as it can be seen for modes 1, 2 and 7, where it shall be annotated that the correlation of the eigenvector no. 7 with respect to the corresponding experimental data reveals to be high already for the initial model (initial $MAC_{7,7}$=0.92).

However, for the 6th eigenfrequency and eigenvector no improvement could be achieved. The reasons might lie in the fact that there is no parameter combination possible which affects an improvement of the fit with respect to all 14 target values defined by the first 7 modal frequencies and mode shape vectors. Only a revision of the model itself might lead to the situation where the

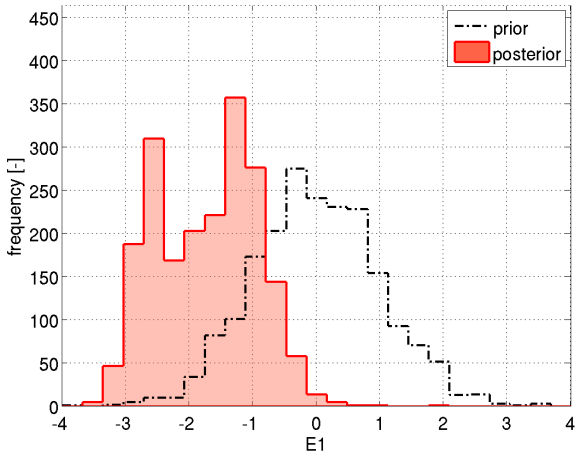


Figure 6: Histograms of the prior and posterior samples of the group of Young's moduli of the orthotropic materials (group no. 3 in Tab. 1)

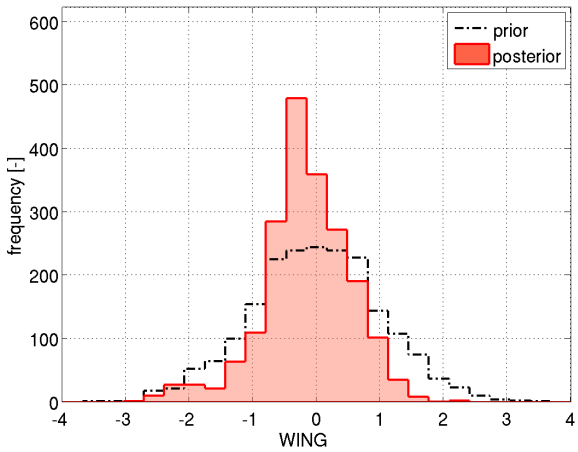


Figure 7: Histograms of the prior and posterior samples of the group of stiffnesses of the joints between wings and main structure (group no. 14 in Tab. 1)

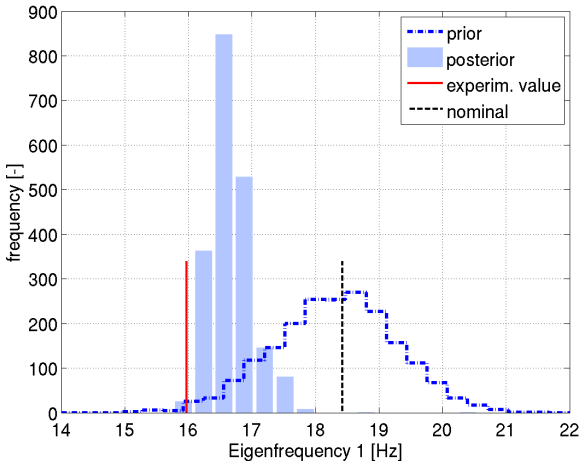


Figure 8: Prior (dashed-dotted line) and posterior (shaded bars) histograms of the 1st eigenfrequency with experimental value (solid line) and nominal value (dashed line)

prior distributions span the full solution space, meaning that posterior samples provoke a high correlation with all targets. As opposed to the first numerical example, where a perturbed model is used for the generation of the target modal data, the present example uses real experimental data and hence a fit with respect to all targets might not be possible without revising the FE-model itself.

### 5.6 Computational aspects

In the first example, the most time-consuming task of the updating algorithm, namely the parts involving eigensolutions, have been parallelized. In the present example, the eigensolution of the full FE-model is replaced by an approximate relation at low computational costs which is given by a neural network for each modal property. If considering that on the above described dual quad-core Xeon server *i)* the replacement of the nominal parameter values $\theta_{\text{nom}}$ by the current value $\theta$ in the FE-input file, the normal mode analysis of the full model performed with MSC.Nastran and the import of the modal quantities into Matlab [26] requires 220 sec (see Appendix A for details on the interaction of Matlab with MSC.Nastran), *ii)* the updating process of the present model involves approximately 32 iterations $\times$ 2,000 eigensolutions and *iii)* the remaining part of the updating process lasts for about 96 min, then the total time amounts up to a theoretical value of

$$t_{\text{full}} = 64,000 \cdot 220\,\text{sec} + 96 \cdot 60\,\text{sec} \approx 160\,\text{days}.$$

In the present example, the computational time of 220 sec of a normal mode analysis of the full FE-model is replaced by the evaluation of the neural networks which takes 0.0014 sec. Hence, in this way the analysis time can be remarkably reduced to

$$t_{\text{NN}} = 64,000 \cdot 0.0014\,\text{sec} + 96 \cdot 60\,\text{sec} \approx 100\,\text{min}.$$

However, it shall be noted that in addition 2,000 calibration samples have been generated (see Sec. 5.3), which require evaluations of the full FE-model lasting for a total time of approx-

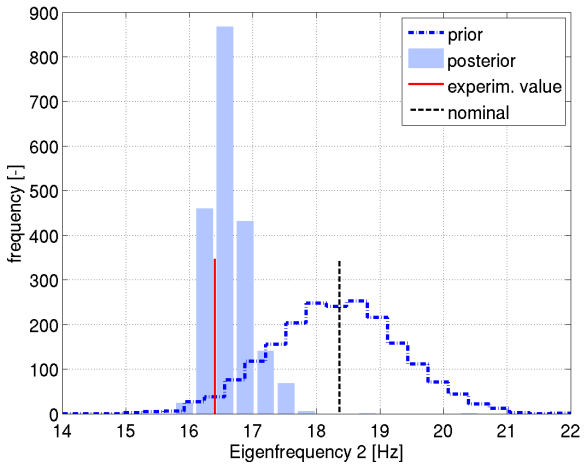


Figure 9: Prior (dashed-dotted line) and posterior (shaded bars) histograms of the 2nd eigenfrequency with experimental value (solid line) and nominal value (dashed line)

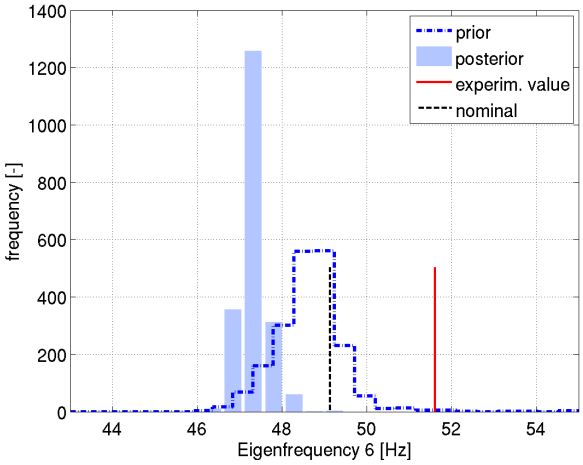


Figure 10: Prior (dashed-dotted line) and posterior (shaded bars) histograms of the 6th eigenfrequency with experimental value (solid line) and nominal value (dashed line)

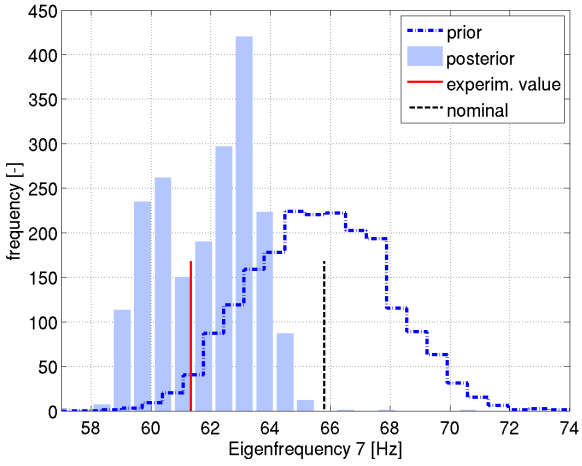


Figure 11: Prior (dashed-dotted line) and posterior (shaded bars) histograms of the 7th eigenfrequency with experimental value (solid line) and nominal value (dashed line)

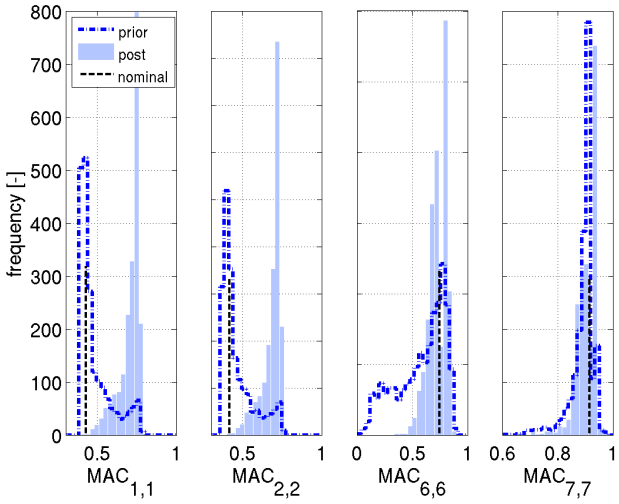


Figure 12: Prior (dashed-dotted line) and posterior (shaded bars) histograms of the diagonal terms of the MAC matrix corresponding to modes no. 1, 2, 6 and 7 and nominal values (dashed lines)

imately 5 days if performed sequentially (see Appendix A for the interaction with 3rd party software).

## 6 CONCLUSIONS

In this manuscript, the basic steps of model updating within the Bayesian framework using modal data have been summarized and strategies for reducing the analysis time are proposed. The numerical example shows the applicability of the Bayesian updating procedure on complex aerospace structures. It demonstrates that ill-conditioned inverse problems in the high-dimensional parameter space can be tackled and that the limited, incomplete data can be used for reducing the initial uncertainty about the adjustable parameters. As a remedy for the large computational efforts of model updating the establishment of a surrogate model has been proposed which approximates the modal properties at a low computational cost. In this way, model updating of a finite element model of a full satellite structure of a size of approximately 360,000 DOFs becomes feasible as shown in the numerical example.

## ACKNOWLEDGEMENTS

This research was partially supported by the European Space Agency (ESA) under Contract No. 20829/07/NL/EM, which is gratefully acknowledged by the authors. The authors thank Thales Alenia Space Italy for the FE-model of the GOCE satellite and the experimental modal data. The first author is a recipient of a DOC-fForte-fellowship of the Austrian Academy of Science at the Institute of Engineering Mechanics (University of Innsbruck).

## REFERENCES

[1] European Cooperation for Space Standardization. Space engineering: Modal survey assessment, *ECSS-E-ST-32-11C*, 2008.

[2] The American Institute of Aeronautics and Astronautics. Guide for the verification and validation of computational fluid dynamics simulations, *AIAA Standards Series (G-077)*, 1998.

[3] The American Society of Mechanical Engineers. Guide for verification and validation in computational solid mechanics, *ASME V&V* (10), 2006.

[4] D. Göge, M. Link, Assessment of computational model updating procedures with regard to model validation, *Aerospace Science and Technology* 7 (2003) 47–61.

[5] A. Calvi, S. Garcia de Paredes, N. Roy, Y. Lefevre, On the development of a stochastic approach for the validation of spacecraft structural dynamic models, in: *Proceedings of the European Conference on Spacecraft Structures, Materials and Mechanical Testing* (CD-ROM), Toulouse, France, 2002.

[6] M. Friswell, J. Mottershead, *Finite Element Model Updating in Structural Dynamics*, Kluwer Academic Publishers, 1995.

[7] A. Girard, N. Roy, *Structural dynamics in industry*, John Wiley & Sons, 2008.

[8] F. Buffe, Application of updating methods on the finite element model of Picard, in: *European Conference on Spacecraft Structures, Materials and Mechanical Testing* (ECSS-MMT 2009; CD-ROM), Toulouse, France, 2009.

[9] D. Göge, M. Link, Results obtained by minimizing natural frequencies and mode shape errors of a beam model, *Mechanical Systems and Signal Processing* 17 (1) (2003) 21–27.

[10] A. Calvi, Uncertainty-based loads analysis for spacecraft: finite element model validation and dynamic responses, *Computers & Structures* 83 (14) (2005) 1103–1112.

[11] J. Beck, L. Katafygiotis, Updating models and their uncertainties. I: Bayesian statistical framework, *Journal of Engineering Mechanics* 124 (4) (1998) 455.

[12] L. Katafygiotis, J. Beck, Updating models and their uncertainties. II: Model identifiability, *Journal of Engineering Mechanics* 124 (4) (1998) 463.

[13] K.-V. Yuen, *Bayesian methods for structural dynamics and civil engineering*, John Wiley & Sons, 2010.

[14] J. Ching, Y.-C. Chen, Transitional Markov Chain Monte Carlo method for Bayesian updating, model class selection, and model averaging, *Journal of Engineering Mechanics* 133 (2007) 816–832.

[15] J. Kleijnen, R. Sargent, A methodology for fitting and validating metamodels in simulation, *European Journal of Operational Research* 124 (1) (2000) 14–29.

[16] D. Rumelhart, J. McClelland, *Parallel Distributed Processing, Exploration in the Microstructure of cognition, Vol. 1 and 2*, MIT Press, Cambridge, MA, 1986.

[17] T. Bayes, An essay towards solving a problem in the doctrine of chances, *Philosophical Transactions of the Royal Society of London* 53 (1763) 370–418.

[18] E. Jaynes, *Probability Theory: The Logic of Science*, Cambridge University Press, 2003.

[19] M. Vanik, J. Beck, S.-K. Au, Bayesian probabilistic approach to structural health monitoring, *Journal of Engineering Mechanics* 126 (2000) 738–745.

[20] N. Metropolis, A. Rosenbluth, M. Rosenbluth, A. Teller, E. Teller, Equations of state calculations by fast computing machines, *Journal of Chemical Physics* 21 (6) (1953) 1087–1092.

[21] W. Hastings, Monte Carlo sampling methods using Markov chains and their applications, *Biometrika* 57 (1) (1970) 97–109.

[22] J. Anderson, *Introduction to Neural Network*, MIT Press, Cambridge, MA, 1995.

[23] C. Bishop, *Neural Networks for Pattern Recognition*, Oxford Univ. Pres, 1995.

[24] S. Nissen, *Implementation of a fast artificial neural network library (fann)*, Tech. rep., Department of Computer Science University of Copenhagen (DIKU) (2003).

[25] MSC.Software Corporation, Santa Ana (CA), USA, MSC.NASTRAN, Version 2007.1.0 (2007).

[26] The MathWork, Natick (MA), USA, Matlab R2009b (2009).

[27] COSSAN-X, COmputational Stochastic Structural ANalysis, Chair of Engineering Mechanics, University of Innsbruck, Innsbruck, Austria, EU (2010).

## A INTERACTION WITH 3RD PARTY SOFTWARE

FE models are defined uniquely by one or more ASCII input files. These files contain the definition of the nodes and elements constituting the model, as well as the structural parameters and boundary and loading conditions in form of fixed numerical values. However, in a stochastic analysis some of these values change, since they are samples from a given probability distribution function. Thus, it is envisioned to automatically manipulate the input files such that in each simulation the respective sample values are inserted into the FE-input file. For this purpose, XML-like tags, called identifiers, are inserted into the master input files in order to define the parameters which have to be changed in each simulation, as shown in Fig. 13. An identifier defines the name of the random variable used within the stochastic analysis, the format in which the number is written into the file as well as the original value of the parameter.

```
MAT1, 1, <cossan name="E" format="%8.2e" original="7.e+10"/>,,

<cossan name="nu" format="%8.2e" original="0.33"/>,

<cossan name="rho" format="%8.2e" original="2000."/>,

2.40E-5, 20.0000
```

Figure 13: Excerpt of a master input file with identifiers

The code used to drive the simulation is COSSAN-X, a software for computational stochastic structural analysis [27]. This code parses the master input files in order to identify the positions and the insertion formats of all variables. In each analysis, these identifiers are replaced by sampled numerical values, obtaining a valid input file which is then used for the finite element analyis (see Fig. 14). It shall be noted that this software is not restricted to a particulare FE-code, but it is applicable to any FE-solver which uses ASCII input files.

```
MAT1, 1, 6.13e+10,, 3.98e-01, 2.22e+03, 2.40E-5, 20.0000
```

Figure 14: Excerpt of a stochastic analysis input file with sampled values.